Journal of Theoretical and Applied Physics (JTAP), Vol.16, No. 4, 162237 (1-6), 2022
Received 17 June 2022 ; Accepted 13 August 2022 ; [http://dx.doi.org/10.30495/jtap.162237]

The spatial damping of electrostatic wave in Hall thruster beam plasma

Saty Prakash Bharti , Sukhmander Singh*

Abstract
The magnetohydrodynamics model is used to investigate the spatial damping in a Hall thruster beam plasma under the effect of thermal motion and electron beam density. Plasma dispersion equation is derived analytically using the normal mode analysis of the small oscillations. The dispersion equation is solved numerically to find out the damping modes in a Hall thrusters plasma. The damping length shows dependence on the radial magnetic field, beam density, ion density, electron drift velocity, collision frequency, electron and ion temperature. We investigated that the damping length increases with ion density and electron-ion temperature, whereas it decreases with the radial magnetic field, beam density, electron drift velocity and collision frequency.

Keywords
Hall thruster, Magnetic field, Electron drift velocity, Damping length, Collision frequency.

Plasma Waves and Electric Propulsion Laboratory, Department of Physics, Central University of Rajasthan, Ajmer, Kishangarh- 305817, India.
***Corresponding author**: sukhmandersingh@curaj.ac.in

1. Introduction

Hall Effect thrusters (HET) are used for electrical propulsion technologies in space due to its long specific impulse and low propellant consumption. HETs are employed to control Earth-orbiting satellites and deep-space robotic vehicles. HET has lifetime from 10,000 hours to 50,000 hours because of its high thrust density.

The inert gas (Xe) of low ionization potential and high atomic weight is used in HET device. Xenon ions are pulled out by external electric field to generate thrust. The negatively charged electrons are emitted thermionically from a hollow cathode in HET. The applied axial electric field and redial magnetic field are normal to each in annular ceramic discharge channel. In HET, the electrons are strongly magnetised in azimuthal direction, while the heavier ions are relatively remains unmagnetized. Both the ions and electrons should rotate under the crossed electric and magnetic fields, but for the given set of parameters, the Larmor radius of the ions remains larger than the length of the channel and ions cant drift in the azimuthal direction and hence simply ejected out by the external electric field. The applied magnetic field extends the residence time period of electrons in the discharge channel by trapping them. The magnetic field lines create a large enough Hall current in the $\mathbf{E} \times \mathbf{B}$ direction. The schematic diagram of Hall thruster is shown in Fig. 1.

HET support a wide range of plasma instabilities by several energy sources (inhomogeneity in plasma and magnetic field) [1–4]. The plasma oscillations and the instabilities control the mobility of charge and transport phenomena in these type of devices. Petronio et al. have used analytical and PIC simulation approach to obtain the growth rate of modified two-stream instability, which depends on plasma density and azimuthal length in Hall thruster [5]. Mikellidesa and Ortega used analytical and numerical approach to model the dispersion relation for lower hybrid and modified two-stream instability in a inhomogenous collisional plasma. It is summarised that the wavenumber and electron/ion temperature increases the growth rate of the instability [6]. The spatial damping is the reduction in the amplitude of the wave with axial position. In other words, spatial damping length is the distance over which the waveamplitude drops to 1/e times of its original amplitude. It can be related to the nonuniformity rate of the plasma density profile or the density scale length of plasma.The literature review reveals that the performance of the Hall thruster depends on the profiles of the plasma density and its performance is maximum, when density scale length of plasma is minimum.The spatial damping of the wave means the release of energy or the weak coupling of free energy to the oscillations, which will not alter the movement of the ions and hence, the thrust is expected to be higher, leading to higher efficiency. Carbonell et al. studied the effect of flows on the damping of non-adiabatic magnetohydrodynamic waves in a magnetised unbounded thermal and slow wave of plasma. It is highlighted that the changes in the time periods of the flow, alter the damping per period of the different waves [7].

Carbonell et al. reported that the spatial damping length for the adiabatic waves in fully ionized ideal plasma is found to 10^{23} meter, whereas in case of non-adiabatic plasma it is 10^{19} meter. Its value decreased to 10^4 meter for the case of non- adiabatic thermal wave in fully ionized ideal plasma [8]. Moortel et al. calculated the behaviour of slow magneto-acoustic wave damping and propagation modes under the effect of compressive viscosity in a homogeneous low-β plasma [9,10]. Pontieu

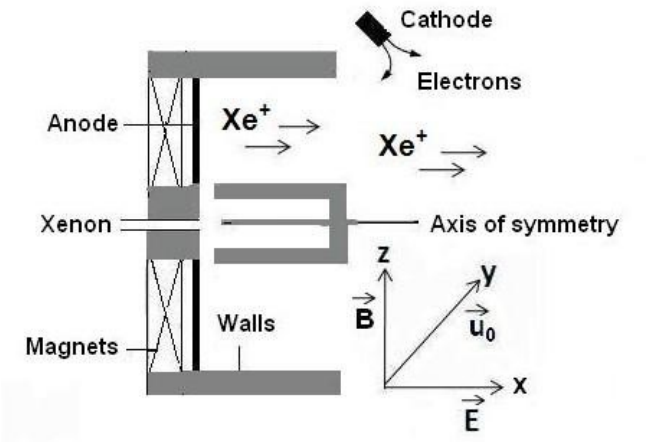

Figure 1. Schematic diagram of a Hall thruster

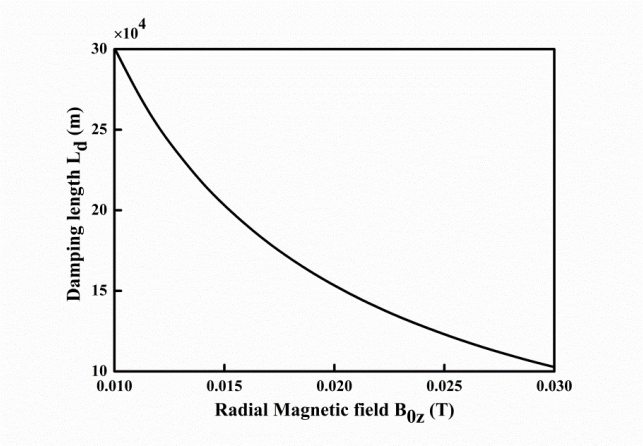

Figure 2. Variation of damping length L_d with radial magnetic field in the plasma having Xeions (mass=131 amu). Here $n_{e0} \approx n_{i0} = 10^{18}$/ m^3, $n_{b0} = 10^{17}$/m^3, $T_e = 5$ eV, $T_i = 1$ eV, $v_{i0} = 10^4$ m/s, $v_{e0} = 10^6$ m/s, $v_{b0} = 10^6$ m/s, $\nu = 10^6$ /s,

et al. calculated the damping of mode oscillations due to collision between neutrals and ions in the various solar features coronal Alfven wave in ionized chromosphere. The less and colder dense feature shows the strongest damping sunspots penumbra and sunspots umbra. The hot feature shows weakest damping for a given coronal Alfven wave frequency. The ionized chromospheric damping leads to enhanced foot point losses [11]. Singh et al. investigated that the linear magnetoacoustic waves exhibit strong damping in fast and slow modes. It is seen that the Kraichnan turbulence dominates for longer wave periods ($10^3 - 10^5$ s) and short wave periods ($10^{-7} - 10^2$ s) [12].

Tanenbaum et al. used normal mode oscillations for small amplitude in a homogeneous medium for a wave and magnetic field propagates in the same direction and the wave propagation direction and magnetic field are perpendicular to each other [13]. In the presence of collisions and ionisation, the electrostatics waves become unstable due to azimuthal drift of electrons [14]. Chesta et al. calculated the frequency and growth rate of azimuthally and axial propagating turbulences in Hall thruster. They have also calculated ionization-related low-frequency instability [15]. The electron $\mathbf{E} \times \mathbf{B}$ drift instability is studied using 1D Particle-in-Cell technique in a Hall thruster. The electrons cross-field mobility increase due to variations in electron density and electric field. It varies with ion mass and plasma density [16]. The virtual cathode installed outer side of the thruster used to neutralize the positively charged surface of the thruster. The fast energetic electrons travel inside the channel and may increase the electrons density, called electron beam density. Bharti et al. investigated the instabilities in beam plasma, the growth rate increases linearly with electron collision but it decreases electron density [17, 18]. Malik et al. studied the Rayleigh–Taylor instability and derived the analytical condition for the growth rate of instability [19]. The electromagnetic [20] and electrostatic instabilities supported by Hall thrusters have been discussed in the references [21–28]. Near the plume regions in HET, Boeuf et al. have used 2D axial-azimuthal PIC simulation of the $\mathbf{E} \times \mathbf{B}$ electron drift instability [29]. The damping and propagation of slow magnetohydrodynamics waves [30] and the magnetoacoustic waves are discussed in coronal plasma [31]. Malik et al. used the concept of tapered coils to generate higher current density and high thrust performance for space propulsion vehicles [32,33]. Computational fluid dynamics is used to compare the aerodynamic properties as shear stress, temperature and nature of pressure distributions on the F16, F22, Rafale and Eurofighter combat aircraft surface [34,35].

2. Mathematical model of problem

Let us consider a HET having ions, electrons and electron beam. Electrons are magnetized in the presence of magnetic field $\mathbf{B} = B\hat{z}$ (z-axis along the radius of thrusters). The axial electric field $\mathbf{E} = E\hat{x}$ (x-axis along the axis of thruster) accelerates the particles. Below, we write the magnetohydrodynamics equations

$$\frac{\partial n_\alpha}{\partial t} + \nabla \cdot (\mathbf{v}_\alpha n_\alpha) = 0 \tag{1}$$

Here the species α =ion (i), electron (e) and electron beam (b)

$$\frac{\partial \mathbf{v}_i}{\partial t} + (\mathbf{v}_i \cdot \nabla)\mathbf{v}_i = \frac{e\mathbf{E}}{m_i} - \frac{T_i \nabla n_i}{m_i n_i} \tag{2}$$

$$\frac{\partial \mathbf{v}_e}{\partial t} + (\mathbf{v}_e \cdot \nabla)v_e = -\frac{e(\mathbf{E} + \mathbf{v}_e \times \mathbf{B})}{m_e} - \frac{T_e \nabla n_e}{m_e n_e} - \nu \mathbf{v}_e \tag{3}$$

$$\frac{\partial \mathbf{v}_b}{\partial t} + (\mathbf{v}_b \cdot \nabla)\mathbf{v}_b = -\frac{e\mathbf{E}}{m_b} \tag{4}$$

It is assumed that the dominated waves are presented only in the azimuthal direction as compared to axial direction.

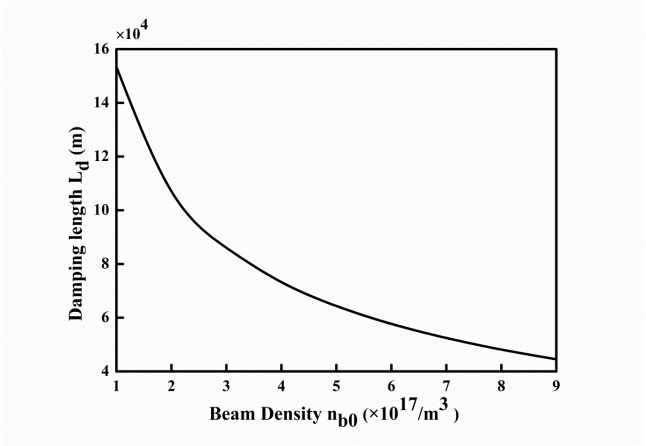

Figure 3. Dependence of damping length with beam density. Here $B_z = 0.02T$ and using the same parameter from Fig.2.

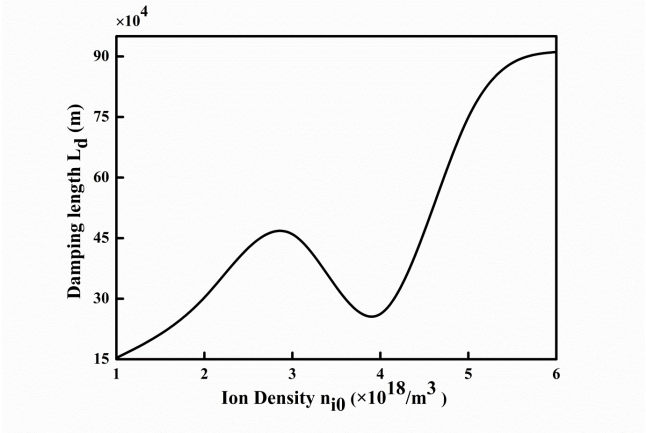

Figure 4. Dependence of damping length with ion density. Here $B_z = 0.02T$ and using the same parameter from Fig.2.

Let the perturbed variables oscillates in the form $A(r,t) = A_0 \exp[i(yk - \omega t)]$. In these equations, n_i is the ion density, n_e is the electron density, n_b is the electron beam density, m_i is the ion mass, the electron mass m_e and electron beam mass $m_b(= m_e)$, v_i is the ion fluid velocity, v_e is the electron fluid velocity, v_b is the electron beam velocity, $\mathbf{E}$ is the electric field, the collision frequency ν, T_i is ion temperature and T_e is electron temperature. We linearized the above equations to find out the velocity components of plasma species. Consider perturbed densities (n_i, n_e and n_b), unperturbed density (n_{i0}, n_{e0} and n_{b0}), perturbed velocity (v_i, v_e and v_b) and unperturbed velocity (v_{i0}, v_{e0} and v_{b0}). The electrons cyclotron frequency defined as $\Omega = eB/m_e$ and the condition $\Omega \gg \omega, kv_{e0}, \nu$ is easily satisfied because the magnetic field is large enough in HET [19-23]. Consider $\mathbf{v}_{i0} = v_{i0}\hat{x}$ is initial drift of ions along the +x direction and neglecting its motion in azimuthal as well as radial direction. Electron beam are also make motion in the +x direction ($\mathbf{v}_b = v_{b0}\hat{x}$) and $\mathbf{E} \times \mathbf{B}$ drift of electrons is in the y–direction ($\mathbf{v}_e = v_{e0}\hat{y}$). The initial drift velocity of electron is denoted by $\mathbf{v}_{e0} = -(E_0/B_0)\hat{y}$. To obtain the x and y component of electron velocities from equations 3, we get

$$v_{ex} = \frac{1}{m\Omega^2}(iek\Omega\phi - \frac{im\Omega kV_{the}^2 n_e}{n_{e0}}) +$$

$$\frac{i\hat{\omega}^2}{m\Omega^3}(ek\phi - \frac{mkV_{the}^2 n_e}{n_{e0}}) \tag{5}$$

$$v_{ey} = \frac{\hat{\omega}}{m\Omega^2}(ek\phi - \frac{mkV_{the}^2 n_e}{n_{e0}}) \tag{6}$$

the perturbed density of electrons is determined as

$$n_e = \frac{en_{e0}k^2\phi(\omega - kv_{e0} - i\nu)}{m_e[\Omega^2(\omega - kv_{e0}) + (\omega - kv_{e0} - i\nu)k^2V_{the}^2]} \tag{7}$$

the perturbed ion density is given by

$$n_i = \frac{en_{i0}k^2\phi}{m_i[\omega^2 - k^2V_{thi}^2]} \tag{8}$$

Finally, the perturbed electron beam density is calculated as

$$n_b = -\frac{en_{b0}k^2\phi}{m_b\omega^2} \tag{9}$$

The obtained perturbed densities are substituted into Poisson's equation $\varepsilon_0\nabla^2\phi = e(n_e - n_i + n_b)$ to obtain the dispersion relation

$$-k^2\phi = \frac{e^2n_{e0}k^2\phi(\omega - kv_{e0} - i\nu)}{m_e\varepsilon_0[\Omega^2(\omega - kv_{e0}) + (\omega - kv_{e0} - i\nu)k^2V_{the}^2]} -$$

$$\frac{e^2n_{i0}k^2\phi}{m_i\varepsilon_0[\omega^2 - k^2V_{thi}^2]} - \frac{e^2n_{b0}k^2\phi}{m_b\varepsilon_0\omega^2} \tag{10}$$

Since, the perturbed potential is non-zero, i.e. $\phi \neq 0$ therefore, we get

$$\frac{\omega_{pe}^2(\omega - kv_{e0} - i\nu)}{\Omega^2(\omega - kv_{e0}) + (\omega - kv_{e0} - i\nu)k^2V_{th}^2} -$$

$$\frac{\omega_{pi}^2}{\omega^2 - k^2V_{thi}^2} - \frac{\omega_{pb}^2}{\omega^2} + 1 = 0 \tag{11}$$

where the plasma frequencies as;

$$\omega_{pe} = (\frac{e^2n_{e0}}{m_e\varepsilon_0})^{\frac{1}{2}}, \omega_{pi} = (\frac{e^2n_{i0}}{m_i\varepsilon_0})^{\frac{1}{2}}, \omega_{pb} = (\frac{e^2n_{b0}}{m_b\varepsilon_0})^{\frac{1}{2}},$$

After simplification of eq. (9), we obtain

$$av_{e0}V_{the}^2V_{thi}^2k^5 - daV_{the}^2V_{thi}^2k^4 + k^3f_1 +$$

$$k^2f_2 - kf_3 + d\omega^4\omega_{pe}^2 + b\omega^3\Omega^2 = 0 \tag{12}$$

The equation (12) is called the dispersion equation under the influences of beam plasma density in the Hall thrusters plasma. Various coefficients of the above equation are given in the Appendix.

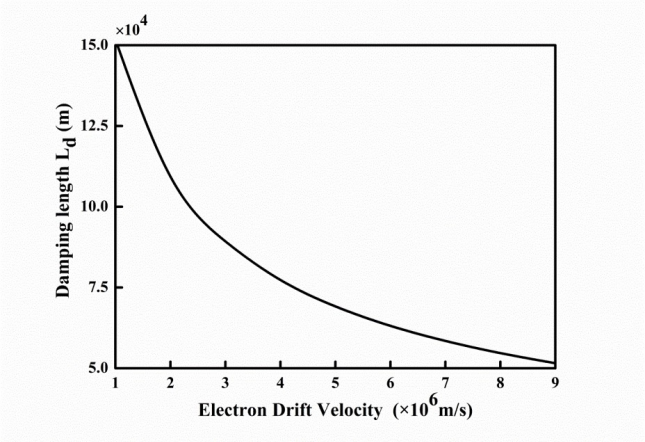

Figure 5. Dependence of damping length with electron drift velocity. Here $B_z = 0.02T$ and using same parameter from Fig.2.

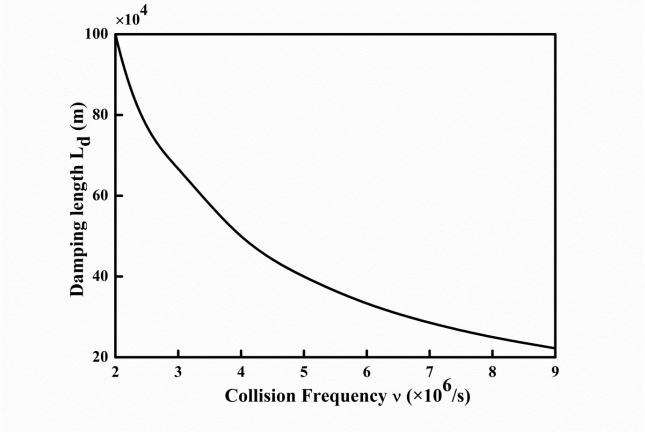

Figure 6. Dependenceof damping lengthwith collision frequency. Here $B_z = 0.02T$ and using same parameter from Fig.2.

3. Graphical analysis and discussion

We consider the frequency ω of the oscillations to be real for the given set of parameters. To seek the complex solutions of the wavenumber, we substitute $k = k_r + ik_i$. The damping length is expressed by $L_d = 1/k_i$ and the damping length per wavelength is $L_d = \lambda$. The dispersion relation is solved numerically to obtain the roots of the equation [12]. Typically, parameters employed in Eq. [12] are, radial magnetic field $B_{0z} = 0.01 - 0.02T$, beam density $n_{b0} = 1 \times 10^{17} - 9 \times 10^{17}$/ m^3, ion density $n_{i0} = 1 \times 10^{18} - 6 \times 10^{18}$/ m^3, electron drift velocity $v_{e0} = 1 \times 10^6 - 9 \times 10^6$ m/s, collision frequency $\nu = 2 \times 10^6 - 9 \times 10^6$ m^3, electron temperature $T_e = 1 - 10$ eV, ion temperature $T_i = 1 - 10$ eV and the thruster diameter 4-10 cm [36–41].

In Fig.2, we have plotted the damping length with different values of radial magnetic field. It is observed that damping length decreases with larger values of the magnetic field. The maximum damping length is found to 30×10^4 meter at $0.01T$ magnetic field and then it falls exponentially to one-third (falls 67 %) of its initial value, when the magnetic field increases to three times.

Fig.3 illustrates that the damping length falls exponentially with higher beam density. It is found that the damping length decreases by 75 %, when the beam density increased by nine-times of its initial value. The maximum damping length is observed to 15.33×10^4 m, at the beam density 1×10^{17}/ m^3. The damping length shows oscillatory behaviour with ion density and its amplitude increases (∼500 %) with higher ion density as shown in Fig.4. The damping length shows peak at resonance, when ion density varies from 1×10^{18}/ m^3 to 6×10^{18}/ m^3.

Fig. 5 represent the variation of damping length with electron drift velocity. It is observed that in the presence of stronger electron drift velocity, the damping length decreases by 75 %. The dependence of the damping lengthwith collision frequency has been shown in Fig. (6). The damping length falls (∼80%) exponentially, when the collision frequency increases.

The effect of electron and ion temperature on the damping length are shown in Fig.7 and Fig.8 respectively. The damping length increased by 440% with the higher electron temperature, but it increases slowly (66%) with ion temperature. Finally, this would be worth mentioning that the magnetic field plays a vital role in controlling the oscillations and hence, its profile is expected to have implications on the thrust and efficiency of the Hall thrusters. In this direction, to realize better efficiency, one can work towards the calculations of growth rate under the effect of magnetic field having a similar kind of field profile used elsewhere [42–48].

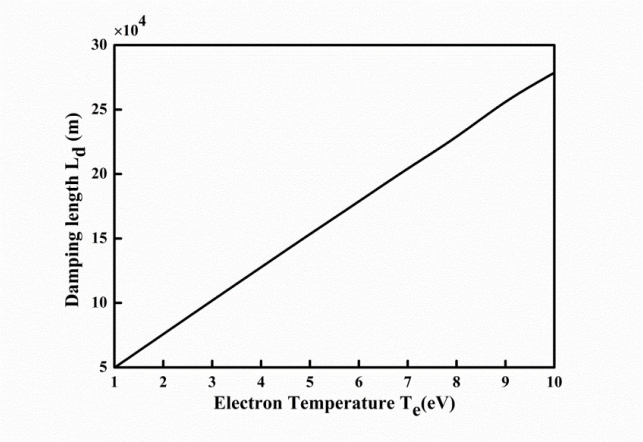

Figure 7. Dependenceof damping length with electron temperature. Here $B_z = 0.02T$ and using same parameter from Fig.2.

4. Conclusion

We obtained the dispersion relation using magnetohydrodynamics approximation and solved it numerically to observe

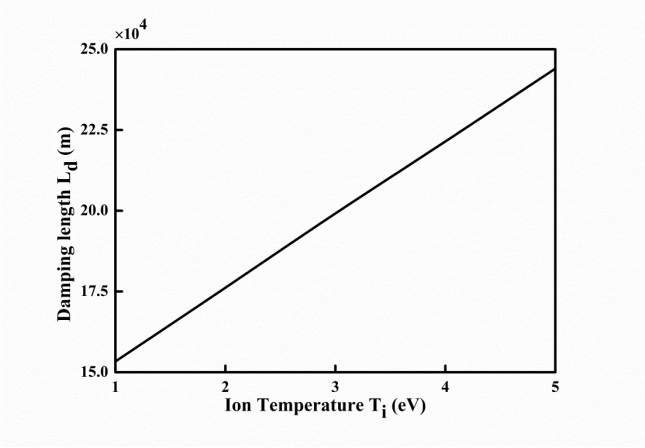

Figure 8. Dependenceof damping length with ion temperature. Here $B_z = 0.02T$ and using same parameter from fig.2.

the variations of damping length for different values of the parameters. The spatial damping length is determined in the Hall thruster collisional plasma under the influence of various effects. The resistive coupling of the waves leads to the growth rate of instability due to the $\mathbf{E} \times \mathbf{B}$ drift. The damping length decreases with the magnetic field, beam density, collision frequency and drift velocity of electrons but it increases with electron and ion temperature.

Appendix: Here the coefficients used in (10) are given as below

$$f_1 = a\Omega^2 v_{e0} V_{thi}^2 - a\omega^2 v_{e0} V_{the}^2 + c\omega^2 v_{e0}$$

$$f_2 = da\omega^2 V_{the}^2 - dc\omega^2 - a\omega\Omega^2 V_{thi}^2$$

$$f_3 = b\omega^2\Omega^2 v_{e0} + \omega^4 \omega_{pe}^2 v_{e0}$$

And other coefficient's constant values are

$$a = \omega^2 - \omega_{pb}^2$$

$$b = a - \omega_{pi}^2$$

$$c = \omega_{pi}^2 V_{the}^2 + \omega_{pe}^2 V_{thi}^2$$

$$d = \omega - i\nu$$

Acknowledgements:
The University Grant Commission (UGC), New Delhi, India is thankfully acknowledged for providing the financial support to continue the research.

Conflict of interest statement:
The authors declare that they have no conflict of interest.

References

[1] D. O. Reilly, G. Herdrich, and D. F. Kavanagh. *Aerospace*, **8**:22, 2021.

[2] J. Zubair. *AIAA Propulsion and Energy Forum*, :3628, 2020.

[3] E. Y. Choueiri. *Physics of Plasmas*, **8**:1411, 2001.

[4] E. T. Dale and B. A. Jorns. *Journal of Applied Physics*, **130**:133302, 2021.

[5] F. Petronio, A. Tavant, T. Charoy, A. A. Laguna, A. Bourdon, and P. Chabert. *Physics of Plasmas*, **28**:043504, 2021.

[6] I. G. Mikellidesa and A. L. Ortega. *Journal of Applied Physics*, **129**:193301, 2021.

[7] M. Carbonell, J. Terradas, R. Oliver, and J. L. Ballester. *Astronomy and Astrophysics*, **460**:573, 2006.

[8] M. Carbonell, P. Forteza, R. Oliver, and J. L. Ballester. *Astronomy and Astrophysics*, **1515**:A8, 2010.

[9] I. D. Moortel and A. W. Hood. *Astronomy and Astrophysics*, **408**:755, 2003.

[10] I. D. Moortel and A. W. Hood. *Astronomy and Astrophysics*, **415**:705, 2004.

[11] B. D. Pontieu, P. C. H. Martens, and H. S. Hudson. *The Astrophysical Journal*, **558**:859, 2001.

[12] K. A. P. Singh, B. N. Dwivedi, and S. S. Hasan. *Astronomy and Astrophysics*, **473**:931, 2007.

[13] B. S. Tanenbaum. *Physics of Fluids*, **4**:1262, 1961.

[14] H. K. Malik and S. Singh. *Physics of Plasmas*, **20**:052115, 20131.

[15] E. Chesta, N. B. Meezan, and M. A. Cappelli. *Journal of Applied Physics*, **89**:03099, 2001.

[16] Z. Asadi, F. Taccogna, and M. Sharifian. *Frontiers in Physics*, **7**:140, 2019.

[17] S. P. Bharti, S. Singh, S. Kumar, and S. Meena. *Jnanabha*, **51**:114, 2021.

[18] S. P. Bharti and S. Singh. *Journal of Astrophysics and Astronomy*, **43**:1, 2022.

[19] H. K. Malik, J. Tyagi, and D. Sharma. *AIP Advances*, **9**:055220, 2019.

[20] S. Singh and H. K. Malik. *IEEE Transactions on Plasma Science*, **39**:1910, 2011.

[21] S. Singh and H. K. Malik. *Journal of Applied Physics*, **112**:013307, 2012.

[22] J. Tyagi, S. Singh, and H. K. Malik. *Journal of Theoretical and Applied Physics*, **12**:39, 2018.

[23] S. Singh and S. P. Bharti. *AIP Conference Proceedings*, **2220**:130060, 2020.

[24] O. P. Malik, S. Singh, H. K. Malik, and A. Kumar. *Journal of Theoretical and Applied Physics*, **9**:75, 2015.

[25] H. K. Malik and S. Singh. *Physical Review E*, **83**:036406, 2011.

[26] S. S. Singh, Jyoti, and K. P. Misra. *Plasma Research Express*, **4**:025006, 2022.

[27] S. Pachauri, Jyoti, and K. P. Misra. *Plasma Research Express*, **4**:025004, 2022.

[28] J. Chaudhary. *Contributions to Plasma Physics*, **56**:113, 2016.

[29] J. P. Boeuf and L. Garrigues. *Physics of Plasmas*, **25**:061204, 2018.

[30] N. Kumar, A. Kumar, and K. Murawski. *Astrophysics and Space Science*, **361**:1, 2016.

[31] N. Kumar, P. Kumar, S. Singh, and A. Kumar. *Journal of Astrophysics and Astronomy*, **29**:243, 2008.

[32] L. Malik, M. Kumar, and I. V. Singh. *IEEE Transactions on Plasma Science*, **49**:7, 2021.

[33] L. Malik. *Propulsion and Power Research*, **11**:171, 2022.

[34] L. Malik and A. Tevatia. *Defence Science Journal*, **71**:137, 2021.

[35] L. Malik, S. Rawat, M. Kumar, and A. Tevatia. *Materials Today: Proceedings*, **38**:191, 2021.

[36] A. Smirnov, Y. Raitses, and N. J. Fisch. *Journal of Applied Physics*, **95**:2283, 2004.

[37] A. Smirnov, Y. Raitses, and N. J. Fisch. *Journal of Applied Physics*, **92**:5673, 2002.

[38] M. K. Scharfe, M. A. Cappelli, and E. Fernandez. *31st International Electric Propulsion Conference (University of Michigan, Ann Arbor, MI, USA)*, **IEPC-129**:1, 2009.

[39] A. Kapulkin, A. Kogan, and M. Guelman. *Acta Astronautica*, **55**:109, 2004.

[40] E. Chesta, C. M. Lam, N. B. Meezan, D. P. Schmidt, and M. A. Cappelli. *IEEE Transactions on Plasma Science*, **29**:582, 2001.

[41] G. J. M. Hagelaar, J. Bareillesa nd L. Garrigues, and J. P. Boeuf. *Journal of Applied Physics*, **93**:67, 2003.

[42] L. Malik and A. Escarguel. *Europhysics Letters*, **124**:64002, 2019.

[43] L. Malik. *Optics and Laser Technology*, **132**:106485, 2020.

[44] L. Malik, A. Escarguel, M. Kumar, A. Tevatia, and R. S. Sirohi. *Laser Physics Letters*, **18**:086003, 2021.

[45] Munish, R. Dhawan, R. Kumar, and H. K. Malik. *Journal of Taibah University for Science*, **16**:725, 2022.

[46] H. K. Malik. *Physics Letters A*, **384**:126304, 2020.

[47] H. K. Malik. *Physics Letters A*, **379**:2826, 2015.

[48] H. K. Malik. *Laser-Matter Interaction for Radiation and Energy*. CRC Press, 1th edition, 2021.